Anomalous Thermal Expansion

DOI: 10.1002/ange.201300619

Negative Thermal Expansion in $LnCo(CN)_6$ (Ln = La, Pr, Sm, Ho, Lu, Y): Mechanisms and Compositional Trends**

Samuel G. Duyker, Vanessa K. Peterson, Gordon J. Kearley, Anibal J. Ramirez-Cuesta, and Cameron J. Kepert**

Negative thermal expansion (NTE) is a comparatively rare phenomenon that is found in a growing number of materials.[1] The discovery of new NTE materials and the elucidation of mechanisms underpinning their behavior is important both in extending the field and enabling tailored thermal expansion properties. NTE has been found throughout a broad family of cyanide coordination frameworks,[2] arising from thermal population of low-energy transverse vibrations of the cyanide bridges, which reduce the average metal–metal distances, and thus the lattice parameters, with increasing temperature. More complex mechanisms have been established in metal–organic framework materials, in which both local and long-range modes contribute to NTE.[3] The low-energy dynamics of metal-based materials are often modeled in terms of rigid unit modes (RUMs), wherein the metal-centered polyhedra are treated as rigid, with only the linkage being flexible.[2a,4]

Most NTE cyanide frameworks are members of two cubic structural types: $Zn(CN)_2$ analogues,[2a,b,5] containing tetrahedral metal centers in the diamondoid topology; and Prussian blue analogues,[6] with octahedral metal centers in the α-Po topology. NTE has recently been observed in a framework of a different structural type: $ErCo(CN)_6$,[7] possessing hexagonal symmetry ($P6_3/mmc$) owing to the combination of ErN_6 trigonal prisms alternating with CoC_6 octahedra. $ErCo(CN)_6$ displays near-isotropic NTE with axial coefficients of thermal expansion (CTEs) $\alpha_a = da/adT = -8\times10^{-6}\,K^{-1}$, $\alpha_c = -9\times10^{-6}\,K^{-1}$ and effective linear CTE, $\alpha_l = 1/3\ dV/VdT = -9\times10^{-6}\,K^{-1}$.[7]

Herein we probe in detail the novel mechanism for NTE in this structure type through a comprehensive approach combining synthesis, structural and dynamic analysis, and modeling. Substitution of other trivalent lanthanoids for Er yields an extended series, $LnCo(CN)_6$, of which representative members have been selected for characterization (Ln = La, Pr, Sm, Ho, Lu, and Y).

Topotactic dehydration of the parent framework hydrates $LnCo(CN)_6{\cdot}nH_2O$ ($n = 4, 5$) yields an extended isostructural series with the trigonal prismatic LnN_6 coordination geometry (Figure 1a, inset), which is a rare example of an isostructural

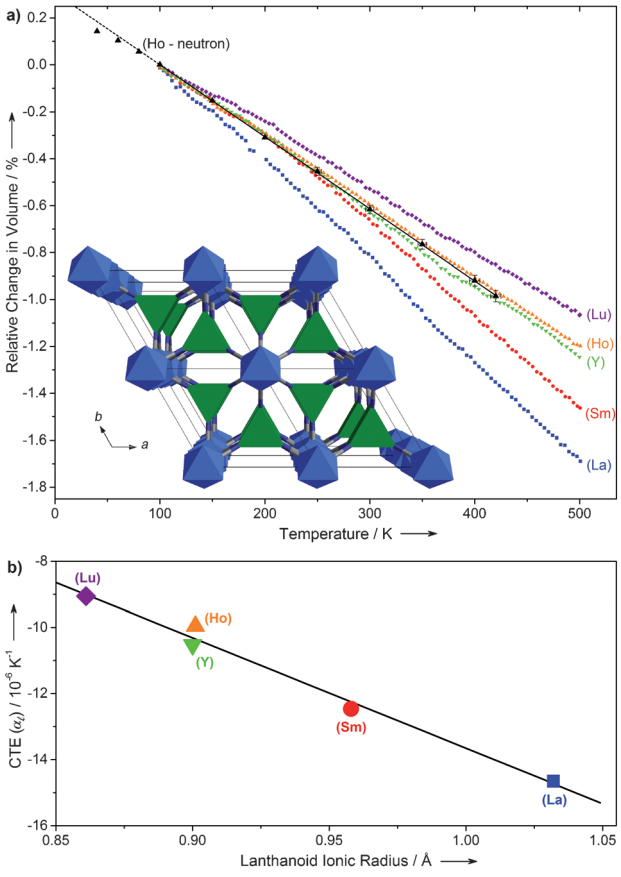

Figure 1. a) Temperature dependence of the unit cell volume relative to the 100 K volume for the $LnCo(CN)_6$ series, determined using XRPD. NPD data for $HoCo(CN)_6$ are plotted, with the linear least-squares fit (solid line) to the 100–420 K range extrapolated (dashed line) to highlight deviation from linearity below 100 K. Inset: the $LnCo(CN)_6$ structure. b) The near-linear relationship between α_l and Ln ionic radius for $LnCo(CN)_6$.[13] Errors are smaller than the data points.

[*] Dr. S. G. Duyker, Prof. C. J. Kepert
School of Chemistry, The University of Sydney
Sydney NSW 2006 (Australia)
E-mail: c.kepert@chem.usyd.edu.au
Dr. S. G. Duyker, Dr. V. K. Peterson, Prof. G. J. Kearley
Australian Nuclear Science and Technology Organisation
Locked Bag 2001 Kirrawee DC NSW 2232 (Australia)
E-mail: vanessa.peterson@ansto.gov.au
Dr. A. J. Ramirez-Cuesta
ISIS, Rutherford Appleton Laboratory
Oxfordshire (UK)

[**] This research was supported by Australian Research Council grants DP120101445 and DP0985611 and fellowships FT100100514 and FF0561456. We acknowledge travel funding provided by the International Synchrotron Access Program (ISAP) managed by the Australian Synchrotron and funded by the Australian Government. S.G.D. acknowledges a postgraduate scholarship funded by the Australian Government and the Australian Institute of Nuclear Science and Engineering. We thank G. J. Halder, K. W. Chapman, P. D. Southon, D. J. Price, Y. Wu, and E. A. Carter for support in experimental work.

Supporting information for this article is available on the WWW under http://dx.doi.org/10.1002/anie.201300619.

series spanning the entire Ln row.[8] This geometry is highly unusual for f-block elements; among several hundred known hexacoordinate lanthanoid complexes that incorporate only non-chelating ligands, only two instances of this geometry exist, both of which are stabilized by ligand–ligand steric effects and differ substantially in their coordination angles from the LnN_6 polyhedra seen here (see the Supporting Information). Such pronounced deviation from the octahedral/pseudo-octahedral stereochemistry typical of hexacoordinate lanthanoid ions[9] suggests that the framework linkage exerts a strong influence on the coordination geometry.

Variable-temperature synchrotron X-ray powder diffraction (XRPD) shows approximately linear volumetric NTE for all $LnCo(CN)_6$ (Ln = La, Sm, Ho, Lu, Y) frameworks in the range 100–500 K (Figure 1 a). The degree of NTE varies with substitution across the f-block, with all but the La analogue displaying near-isotropic behavior (Table 1). The NTE of

Table 1: CTEs for $LnCo(CN)_6$ materials, measured using XRPD (100–500 K) or NPD ([n], 100–420 K).

Material	α_a [$\times 10^{-6}$ K^{-1}]	α_c [$\times 10^{-6}$ K^{-1}]	α_l [$\times 10^{-6}$ K^{-1}]
$LaCo(CN)_6$	−16.58(5)	−10.68(7)	−14.62(4)
$SmCo(CN)_6$	−12.53(14)	−12.31(9)	−12.46(7)
$HoCo(CN)_6$	−10.06(5)	−10.05(7)	−10.05(3)
$HoCo(CN)_6$ [n]	−10.27(9)	−10.32(13)	−10.30(4)
$LuCo(CN)_6$	−9.56(6)	−8.03(7)	−9.05(3)
$YCo(CN)_6$	−10.67(4)	−10.25(6)	−10.53(3)

$LaCo(CN)_6$ is considerably larger than that of ZrW_2O_8 (-9.1×10^{-6} K^{-1})[10] or any of the $M^{II}Pt^{IV}(CN)_6$ materials (-10.02×10^{-6} K^{-1} for M = Cd),[11] and approaches that of $Zn(CN)_2$ (-16.9×10^{-6} K^{-1}).[2a] Neutron powder diffraction (NPD) confirms linear NTE for $HoCo(CN)_6$ between 100 and 420 K (Figure 1 a), with a magnitude close to that measured using X-rays. The NTE is non-linear below 100 K, gradually diminishing with decreasing temperature, indicating depopulation of the low-energy NTE modes.[12]

An almost linear trend relating α_l to the Ln ionic radius[13] (Figure 1 b) is attributed to variation in the framework flexibility accompanying changes in Ln–cyanide bond strength, which is strongly correlated with Ln^{III} ionic radius and Ln–N bond distance. As the ionic radius decreases, the bond strength increases and the framework becomes more thermally rigid, raising the energy of the transverse vibrations and inhibiting their thermal population, resulting in decreased NTE. Conversely, larger ions, such as La, produce a more weakly bonded and commensurately more flexible framework with enhanced NTE. The linear trend seen here contrasts with the more complex behavior for divalent transition-metal substitution in $M^{II}Pt^{IV}(CN)_6$ (M = Mn, Fe, Co, Ni, Cu, Zn, Cd), for which the magnitude of NTE follows the Irving–Williams series of complex stability owing to the influence of crystal-field stabilization energies on M^{II}–N bond strength and for which Jahn–Teller effects are present;[11] for $LnCo(CN)_6$ the absence of significant crystal field effects in the essentially spherical Ln^{III} ions yields fine, continuous control over thermal expansivities by metal substitution. A possible method for finer tuning of the NTE is to employ mixed-lanthanoid solid-solution phases,[14] which are expected to possess CTEs between those of the single-lanthanoid phases.

The slightly larger NTE for Y than Ho is attributed to the slightly weaker bond strength for Y, evident in the different hydration enthalpies of the trivalent ions (Supporting Information).[15] The smaller mass of Y, and any resulting influence on the vibrational energies, is less significant than the bond strength effect. A relationship between framework composition and N-Ln-N bending mode energies (150–250 cm^{-1}) is evident in the Raman spectra (Supporting Information), with the frequencies of peaks in this region increasing with decreasing Ln ionic radius. This trend supports the proposed bond strength basis for the compositional dependence of the NTE. Along with the influence of bond strength on the NTE, there may be a minor compounding effect related to pore size; lanthanoids with smaller ionic radii form phases with smaller pores, which may dampen the cyanide vibrations through increased interaction with the pore walls, similar to the effect of guest water established for Prussian blue analogues.[6a]

Anisotropic atomic displacement parameters (ADPs) give some indication of the directionality of the framework vibrations and may hint at new NTE modes specific to this structure type. The shape and size of displacement ellipsoids reflect the relative magnitudes of dynamic motion in specific directions (in the absence of static disorder) at any given temperature. Variable-temperature measurements elucidate the relative energetics of these modes, with lower-energy modes associated with rapid increases in the ADPs. In the structure of $LuCo(CN)_6$ obtained using single-crystal X-ray diffraction (SCXRD; Figure 2 inset)[16] the shape and orientation of the N ellipsoid is consistent with the presence of transverse vibrations. The C ellipsoid is similar in orientation,

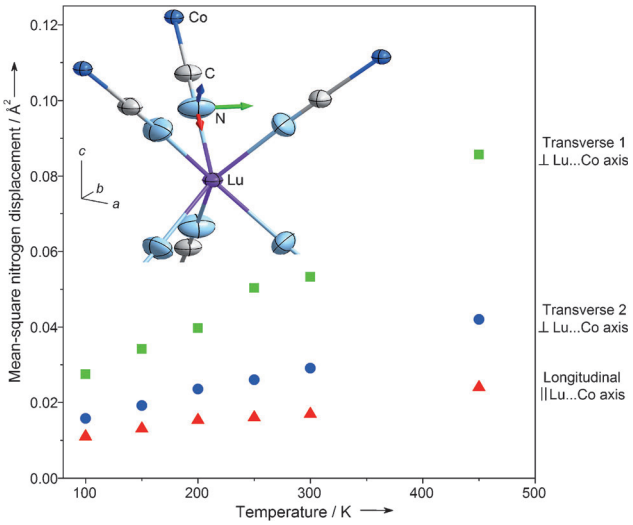

Figure 2. A fragment of the $LuCo(CN)_6$ structure from SCXRD at 450 K (inset), with the shape and orientation of the N displacement ellipsoid (50% probability) suggestive of transverse vibrations. Principal mean-square displacements for N, plotted as a function of temperature, are color-coded to match the arrows in the inset.

but smaller, indicating involvement in similar, but smaller-amplitude, displacements. This suggests a rigid Co-C-N linkage that pivots at the Co, with the smaller amplitude of the C motion arising from its closer proximity to the pivot point; this finding is consistent with the known strong bonding in low-spin octahedral Co^{III} complexes. Given the apparent rigidity of the Co-C-N linkage and the large amplitude of the N displacement, bending of the larger Co-C-N-Lu linkage appears to occur chiefly at the N atom.

The three principal displacements of the N atom exhibit different temperature dependent behaviors (Figure 2). The smallest displacement is oriented almost parallel to the Lu–Co vector and displays the smallest increase with temperature, corresponding to a relatively high-energy longitudinal vibration. The next displacement (transverse 2), increasing intermediately with temperature, is oriented almost perpendicular to the Lu–Co vector, corresponding to a transverse vibration lower in energy than the longitudinal vibration. The largest displacement (transverse 1), also perpendicular to the Lu–Co vector, suggests RUM-type rotation of the LuN_6 trigonal prism on an axis parallel to the *c*-axis. The displacement increases considerably with temperature, indicating that the corresponding transverse motion is relatively large in amplitude, low in energy, and therefore important for NTE. We note that a second, non-RUM twisting mode, in which the top and bottom faces of the prism rotate in opposition about the same axis, is also consistent with this displacement. Temperature-dependent ADPs for $PrCo(CN)_6$ (Supporting Information) show similar behavior to those of $LuCo(CN)_6$.

Averaging the rates of change with temperature of the two transverse N mean-square displacements gives $dU(N\perp_{avg})/dT$ (where U is the displacement), a measure of the temperature dependence of the vibrational amplitude normal to the CN linkage. Use of an averaged value facilitates comparisons with cubic Prussian blue-type materials that have only one unique transverse component in their ADPs. The larger $dU(N\perp_{avg})/dT$ value for $PrCo(CN)_6$ ($14.5(7)\times10^{-5}$ Å^{2}K^{-1}) corresponds to its weaker bonding and increased thermal flexibility compared to $LuCo(CN)_6$ ($11.9(7)\times10^{-5}$ Å^{2}K^{-1}), consistent with the proposed NTE mechanism. $dU(N\perp)/dT$ for $LuCo(CN)_6$ is intermediate between those of the Mn and Cd members of the $M^{II}Pt^{IV}(CN)_6$ series;[11] its CTE also lies between these two compounds. $dU(N\perp_{avg})/dT$ for $PrCo(CN)_6$ is larger than for any $M^{II}Pt^{IV}(CN)_6$ compound. The overall larger values for the $LnCo(CN)_6$ series result from generally weaker M–N bonding for lanthanoids than transition metals, and the possible presence of non-RUM modes, augmenting the bending at the N atom and yielding greater NTE.

As a time-averaged technique, diffraction cannot distinguish between RUM-type rotation and non-RUM twisting vibrations, or prove that the observed ADPs are not simply a result of static disorder. This highlights the need to investigate the dynamics directly. Calculation of an inelastic neutron scattering (INS) spectrum from atomistic simulations is straightforward, providing insight into the modes underlying the measured spectrum.[17] INS spectra for $LnCo(CN)_6$ materials at 100 K, together with the calculated PHONON[18] spectrum for $LaCo(CN)_6$, are shown in Figure 3. The calculated and experimental INS spectra are in good agreement,

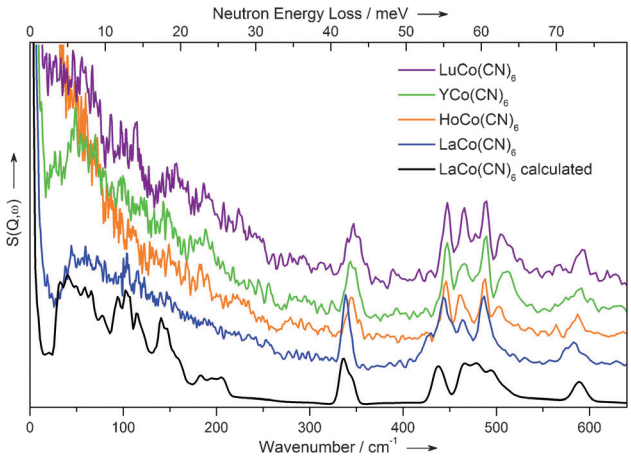

Figure 3. INS spectra, S(Q,ω), for $LnCo(CN)_6$ materials at 100 K (Ln = La, Ho, Y, Lu), and the calculated PHONON spectrum for $LaCo(CN)_6$ at 100 K. Strong scattering at low energies for $HoCo(CN)_6$ arises from the magnetic moment of Ho.

although in the calculated spectrum the broad, low-energy band is shifted to slightly lower energies. This agreement validates a deeper analysis of the modeled dynamics.

The calculation indicates the presence of three relatively low-energy transverse modes below 50 cm^{-1} that are of immediate interest with regard to the NTE (Figure 4 and animations in the Supporting Information). The first of these is a doubly degenerate rocking RUM (25 cm^{-1}), in which the LaN_6 prisms rock in phase and the CoC_6 octahedra rock in the opposite direction. In the second, prism RUM (38 cm^{-1}), the LaN_6 prisms rotate about their axes while the CoC_6 octahedra

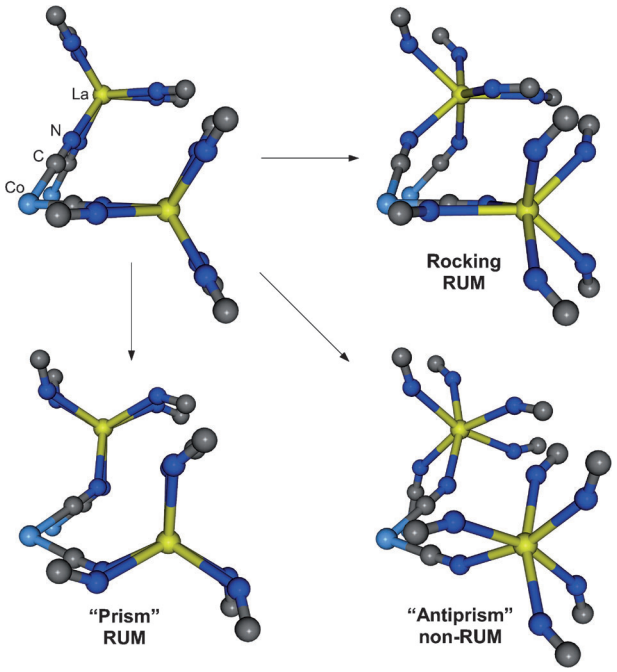

Figure 4. Three low-energy modes contributing to NTE in $LaCo(CN)_6$, viewed along the *c*-axis. See the Supporting Information for animations.

rotate in the opposite direction. The third, antiprism mode (35 cm^{-1}) is the most unusual and confirms the presence of non-RUM behavior noted in the discussion of the ADPs. In this mode, the LaN_6 trigonal prisms twist about their axes such that the top and bottom triangular faces rotate in opposite directions, towards antiprismatic, while the CoC_6 units rotate to accommodate this movement. In all three modes the CoC_6 octahedron is rigid and the Co-C-N linkage remains linear, forming a larger $Co(CN)_6$ octahedral rigid unit that corner-shares with the LaN_6 polyhedron. These modes are consistent with the N ADPs in $LuCo(CN)_6$ and $PrCo(CN)_6$. All three contribute to the larger transverse 1 displacement, while only the doubly degenerate rocking mode contributes significantly to the smaller transverse 2 displacement.

We attribute the non-RUM antiprism mode to the local instability of the trigonal-prismatic lanthanoid coordination geometry,[9a] which is counterbalanced by the stabilizing restraints of the framework's connectivity. The net result of these competing effects appears to be a relatively small energy penalty associated with twisting of the LnN_6 trigonal prisms about the *c*-axis, allowing significant distortion at low thermal energies. Along with the general geometric flexibility of the lanthanoid coordination, this new type of NTE mode likely contributes to the enhanced NTE relative to comparable systems containing only locally optimal coordination geometries, for example the $M^{II}Pt^{IV}(CN)_6$ Prussian blue analogues.[11]

The calculated INS peaks arising from the rocking, prism, and antiprism modes correspond to features in the experimental spectrum between 40 and 70 cm^{-1} (Supporting Information). These values are consistent with the energies of the low-energy modes in $Zn(CN)_2$ and ZrW_2O_8, which lie between about 20 and 70 cm^{-1}.[6b,19] The temperature at which α becomes constant defines an energy range for NTE-contributing modes.[19b] As seen for $HoCo(CN)_6$ using NPD, this occurs at 100 K, corresponding to an energy of 70 cm^{-1}. As the rocking, prism, and antiprism modes are the only modes with calculated energies below this value, we conclude that they are the most significant NTE contributors. Measured spectra for $LaCo(CN)_6$ show temperature dependence in the region corresponding to these transverse modes, with noticeable differences in intensity between the 20 and 100 K spectra at energies below 70 cm^{-1} (Supporting Information). This is commensurate with the reduction of NTE below 100 K seen using NPD.

In conclusion, the $LnCo(CN)_6$ compounds provide a rare example of an isostructural series spanning the entire first-row f-block, and are only the second extended family of materials displaying negative thermal expansion (NTE) at ambient temperature. Early members of the series provide some of the highest coefficients of NTE yet observed, with approximately linear behavior over a broad temperature range without structural transitions. A clear trend relates increasing Ln ionic radius to an increasing NTE magnitude. Our mechanistic analyses indicate the presence of both rigid unit modes (RUMs) and a new non-RUM, the latter associated with the unique coordination geometry and framework topology afforded by the topotactic synthesis. The extra flexibility enabled by the non-RUM is thought responsible in part for the large NTE relative to other hexacyanidometallates.

Finally, we note that considerable potential exists for the extension of this topotactic approach to the design and synthesis of other new NTE materials. Along with producing low atom-density, open framework materials capable of pronounced dynamic transverse distortion, such a route provides significant scope for the stabilization of high energy framework lattices in which competition exists between local metal coordination energies and the minimization of framework strain. In principle, the judicious matching of these energies within an open lattice could lead to very low-energy dynamic framework distortions and even further enhanced NTE.

Received: January 24, 2013
Published online: April 9, 2013

Keywords: coordination frameworks · inelastic neutron scattering · lanthanoids · metal cyanides · rigid unit mode

[1] a) J. S. O. Evans, *J. Chem. Soc. Dalton Trans.* **1999**, 3317 – 3326; b) G. D. Barrera, J. A. O. Bruno, T. H. K. Barron, N. L. Allan, *J. Phys. Condens. Matter* **2005**, *17*, R217 – R252; c) C. J. Kepert, *Chem. Commun.* **2006**, 695 – 700; d) W. Miller, C. W. Smith, D. S. Mackenzie, K. E. Evans, *J. Mater. Sci.* **2009**, *44*, 5441 – 5451; e) K. Takenaka, *Sci. Technol. Adv. Mater.* **2012**, *13*, 013001; f) C. Lind, *Materials* **2012**, *5*, 1125 – 1154.

[2] a) A. L. Goodwin, C. J. Kepert, *Phys. Rev. B* **2005**, *71*, 140301; b) K. W. Chapman, P. J. Chupas, C. J. Kepert, *J. Am. Chem. Soc.* **2005**, *127*, 15630 – 15636; c) A. L. Goodwin, M. Calleja, M. J. Conterio, M. T. Dove, J. S. O. Evans, D. A. Keen, L. Peters, M. G. Tucker, *Science* **2008**, *319*, 794 – 797; d) S. J. Hibble, G. B. Wood, E. J. Bilbé, A. H. Pohl, M. G. Tucker, A. C. Hannon, A. M. Chippindale, *Z. Kristallogr.* **2010**, *225*, 457 – 462.

[3] a) Y. Wu, A. Kobayashi, G. J. Halder, V. K. Peterson, K. W. Chapman, N. Lock, P. D. Southon, C. J. Kepert, *Angew. Chem.* **2008**, *120*, 9061 – 9064; *Angew. Chem. Int. Ed.* **2008**, *47*, 8929 – 8932; b) V. K. Peterson, G. J. Kearley, Y. Wu, A. J. Ramirez-Cuesta, E. Kemner, C. J. Kepert, *Angew. Chem.* **2010**, *122*, 595 – 598; *Angew. Chem. Int. Ed.* **2010**, *49*, 585 – 588.

[4] V. Heine, P. R. L. Welche, M. T. Dove, *J. Am. Ceram. Soc.* **1999**, *82*, 1793 – 1802.

[5] A. E. Phillips, A. L. Goodwin, G. J. Halder, P. D. Southon, C. J. Kepert, *Angew. Chem.* **2008**, *120*, 1418 – 1421; *Angew. Chem. Int. Ed.* **2008**, *47*, 1396 – 1399.

[6] a) A. L. Goodwin, K. W. Chapman, C. J. Kepert, *J. Am. Chem. Soc.* **2005**, *127*, 17980 – 17981; b) K. W. Chapman, M. Hagen, C. J. Kepert, P. Manuel, *Physica B* **2006**, *385*, 60 – 62.

[7] T. Pretsch, K. W. Chapman, G. J. Halder, C. J. Kepert, *Chem. Commun.* **2006**, 1857 – 1859.

[8] a) A. Chatterjee, E. N. Maslen, K. J. Watson, *Acta Crystallogr. Sect. B* **1988**, *44*, 381 – 386; b) M. Seitz, A. G. Oliver, K. N. Raymond, *J. Am. Chem. Soc.* **2007**, *129*, 11153 – 11160.

[9] a) D. L. Kepert, *Inorganic Stereochemistry*, Springer, Berlin, **1982**; b) N. N. Greenwood, A. Earnshaw, *Chemistry of the Elements*, 2nd ed., Butterworth-Heinemann, Oxford, UK, **1997**.

[10] T. A. Mary, J. S. O. Evans, T. Vogt, A. W. Sleight, *Science* **1996**, *272*, 90 – 92.

[11] K. W. Chapman, P. J. Chupas, C. J. Kepert, *J. Am. Chem. Soc.* **2006**, *128*, 7009 – 7014.

[12] a) J. S. O. Evans, W. I. F. David, A. W. Sleight, *Acta Crystallogr. Sect. B* **1999**, *55*, 333 – 340; b) W. I. F. David, J. S. O. Evans, A. W. Sleight, *Europhys. Lett.* **1999**, *46*, 661.
[13] R. D. Shannon, *Acta Crystallogr. Sect. A* **1976**, *32*, 751 – 767.
[14] D. F. Mullica, F. H. Alvarez, E. L. Sappenfield, *J. Solid State Chem.* **1997**, *129*, 12 – 16.
[15] L. R. Morss, *Chem. Rev.* **1976**, *76*, 827 – 841.
[16] Further details on the crystal structure investigation may be obtained from the Fachinformationszentrum Karlsruhe, 76344 Eggenstein-Leopoldshafen, Germany (fax: (+49) 7247-808-666; e-mail: crysdata@fiz-karlsruhe.de), on quoting the depository numbers CSD-425666 to CSD-425677, inclusively.
[17] G. J. Kearley, *Nucl. Instrum. Methods Phys. Res. Sect. A* **1995**, *354*, 53 – 58.
[18] K. Parlinski, PHONON Software (**2005**).
[19] a) R. Mittal, M. Zbiri, H. Schober, E. Marelli, S. J. Hibble, A. M. Chippindale, S. L. Chaplot, *Phys. Rev. B* **2011**, *83*, 024301; b) G. Ernst, C. Broholm, G. R. Kowach, A. P. Ramirez, *Nature* **1998**, *396*, 147 – 149.

